Fachtagung "Lasermethoden in der Strömungsmesstechnik"
7. – 9. September 2010, Cottbus

LIF-MESSUNGEN UND SELBSTÄHNLICHKEITSBETRACHTUNGEN IN EINER STABIL STRATIFIZIERTEN ISOKINETISCHEN TURBULENTEN MISCHUNGSSCHICHT

LIF-MEASUREMENTS AND SELF-SIMILARITY CONSIDERATIONS IN A STABLY STRATIFIED ISOKINETIC TURBULENT MIXING LAYER

J. Fokken, R. Kapulla, G. Galgani, O. Schib, K. Pawa, H.M. Prasser
Labor für Thermohydraulik (LTH), Paul Scherrer Institut (PSI), 5232 Villigen, Schweiz

LIF, Isokinetische Mischungsschicht, Selbstähnlichkeit
LIF, Isokinetic Mixing Layers, Self-Similarity

Abstract

The turbulent mixing of coolant streams of different temperature and density can cause severe temperature fluctuations in piping systems, or in more complex apparatus such as the reactor pressure vessel or the steam generator of a nuclear power plant. Such fluctuations may lead to thermal fatigue in the junctions where mixing occurs.
To study the fundamental turbulent mixing phenomena in the presence of density gradients, co-flow isokinetic water experiments were carried out in a channel with Reynolds Numbers ranging from Re = 5E+03 to 1E+05 at various relative density differences.
Laser induced fluorescence (LIF) was used to visualize the evolution of the concentration field developing downstream of the splitter plate tip for different relative density ratios covering the range from 0 to 10 %. With image analysis procedures it was possible to calculate semi-quantitative mean and rms value concentration fields.
It was found, that for the unstratified case as well as for experiments with moderate density differences up to 5% the width of the mixing zone as depicted by the dye pattern grows almost linearly with downstream distance for the Re-number range considered here, although the patterns of the mixing eddies change considerably. Increasing the density difference further suppresses the mixing zone growth for low Re-numbers almost completely resulting in a step-shaped density interface preserved over a distance of 400 mm. Extracting mean and rms value profiles from the concentration field, self similarity flow characteristics could be proven when plotting the profiles in appropriate similarity variables.

1. Introduction

The design-lifetime of most nuclear power plants (NPP) worldwide in operation is 40 years. Some of these facilities in the world are already close to the end of this period. The licensees of these facilities wish to extend their lifetimes up to 60 or more years, provided that up-to-date security requirements are met and maintained. One important issue regarding the lifetime extension is the monitoring and assessment of thermal fatigue. Thermal fatigue is a mechanism which results in significant degradation of the mechanical properties of a material exposed to cyclic thermal stresses, thereby reducing its ability to support mechanical loads. A component may fail before its design lifetime due to thermal fatigue. Typical components susceptible to thermal fatigue are junctions, locations where two fluids of different temperatures and consequently, different densities, mix. Several T-Junction experiments (Chapuliot et al 2005, Metzner 2004, Walker et al 2009) have been carried out to study the mechanisms

leading to pipe cracks. However, one still encounters difficulties in predicting the location of failures with numerical codes in such mixing zones. The water mixing experiments in the GEMIX-Facility (Generic Mixing Experiment) are dedicated to the basic mechanisms of turbulent mixing in the presence of temperature and/or density gradients under isokinetic mixing conditions. Laser Induced Fluorescence (LIF) is used to measure the concentration field, which provides information about the mixing process in the flow direction. Also used in the experiment, but not presented in this article, are Wire Mesh Sensors (WMS), Prasser et al 1998, to study the mixing process over the cross sectional area normal to the flow direction, as well as Particle Image Velocimetry (PIV) for measurement of the velocity field. The interested reader may refer to Kapulla et al 2009, Fokken et al 2009 and Fokken et al 2010.
In this paper, the experimental and LIF setup are first briefly introduced. The second section consists of a qualitative discussion of the flow inside the GEMIX-Facility for various inlet bulk velocities and density differences. Finally, the third section presents a semi-quantitative analysis and the introduction of similarity variables to describe the results in further detail.

2. Experiment

The GEMIX-Facility is designed to investigate the effect of density gradients as well as of viscosity and temperature gradients on turbulent mixing. The set-up of the principal system components is pictured in Figure 1.

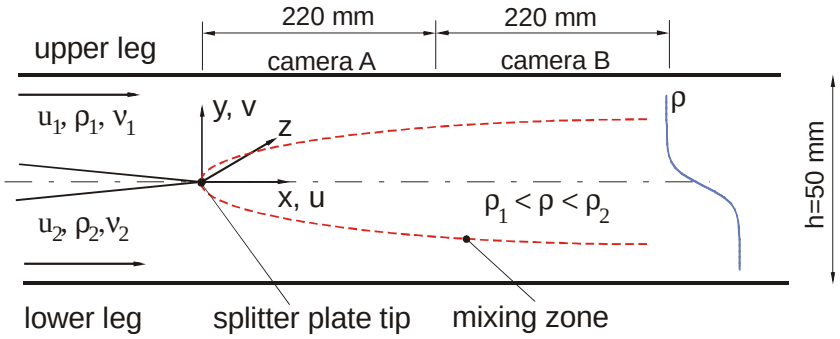

Figure 1: Principal sketch of GEMIX-Facility primary components

The GEMIX-Facility is designed to accommodate temperature differences up to $\Delta T = 50$ K and density differences up to $\Delta\rho = 15\%$. The test section consists of an acrylic glass channel with square cross-section (50x50 mm). It is fed from two storage tanks, each having a volume of 2000 L. The storage capacity allows for experiments of up to 15 minutes with a maximum velocity of $u_0 = 1$ m/s. The loop is open, indicating that the water is purged to the drain after mixing. The origin of the coordinate system describing the flow field is located at the splitter plate tip in the centre of the channel, Figure 1.
The two liquid streams are initially separated by a splitter plate. This part of the test section is called the flow conditioning section. Inside the flow conditioning section both streams pass through honeycombs and grids such that the velocity profiles at the splitter plate tip are mostly free from rotational components, have small boundary layers and therefore have flat and equal profiles at the end of the splitter plate. As the flows pass the splitter plate tip, the streams interact with one another and form the mixing zone. The pumping station driving the test section establishes equal initial velocities for both streams, also referred to as isokinetic conditions $u_1 = u_2 = u_0$, in the range from 0.1 to 1.0 m/s. This velocity range corresponds to Reynolds numbers from Re = 5.000 to Re = 100.000.
The density ρ, and the kinematic viscosity of both streams, ν, can be adjusted by varying the temperature and/or adding sucrose to the fluid in one leg to increase the density difference. Density differences of up to 1.5% may be adjusted by heating one of the fluids. For density differences above 1.5% sucrose is added. The addition of high amounts of sucrose can

cause considerable change in the kinematic viscosity. To minimize this effect, it is necessary to heat the sucrose solution to a temperature where the kinematic viscosity is comparable to that of the pure water in the other leg. To generate a 10% density difference with respect to pure demineralised water at 20℃, a sucrose solution of nearly 30-mass % is required. In order to match the kinematic viscosities of both streams, a sucrose solution temperature of approximately 50℃ is required. The physical fluid properties of the sucrose solutions as well as of water are given in Table 1. For example, conducting experiments with a stable density difference of 5% the lower stream consists of tap water with a temperature of T_2=43℃ where 15-mass % sucrose was added, while for the upper stream demineralised water at T_1=23℃ is used.

Fluid	**ν [10^{-6} m^2/s]**	**ρ [kg/m^3]**	**$\Delta\rho_{H2O(20°C)}$ [%]**
Demineralised water (20℃)	1.00	998	0
Tap water (50℃)	0.56	988	1
Tap water, 8.5 mass-% sucrose cont. 33℃	0.89	1029	3
Tap water, 15 mass-% sucrose cont. 43℃	0.88	1051	5
Tap water, 26 mass-% sucrose cont. 46℃	1.15	1098	10

Table 1: Dependence of fluid properties for water and sucrose solution

3. LIF-Setup and Experimental Program

One technique to monitor the mixing process in the GEMIX-Facility is Laser Induced Fluorescence (LIF). For the LIF recording a DANTEC PIV system is used, consisting of two identical CCD cameras (Kodak MegaPlus ES 1.0, 1016x1008 pixel) and a system hub to run both cameras simultaneously with a maximum frequency of 15 Hz.

Exp. No.	U_0 m/s	T_1 ℃	T_2 ℃	Re_1 [-]	Re_2 [-]	ρ_1 kg/m^3	ρ_2 kg/m^3	$\Delta\rho$ %	Sucrosecont. mass-%
N237	0.2	21	21	7000	7000	998	998	**0**	0
N239	0.4	21	21	13000	13000	998	998	**0**	0
N240	0.8	21	21	27000	27000	998	998	**0**	0
N248	0.2	19	50	12000	7000	988	998	**1**	0
N249	0.4	19	50	24000	13000	988	998	**1**	0
N250	0.8	19	50	49000	27000	988	998	**1**	0
N245	0.2	23	33	7000	7000	998	1029	**3**	8.5
N246	0.4	23	33	13000	15000	998	1029	**3**	8.5
N247	0.8	23	33	27000	30000	998	1029	**3**	8.5
N242	0.2	20	41	6000	8000	998	1051	**5**	15
N243	0.4	20	41	13000	15000	998	1051	**5**	15
N244	0.8	20	41	27000	30000	998	1051	**5**	15
N253	0.4	16	46	13000	12000	998	1099	**10**	26
N254	0.2	16	46	7000	6000	998	1099	**10**	26
N255	0.8	16	46	27000	23000	998	1099	**10**	26

Table 2: Initial conditions for the experiments conducted

Both cameras are positioned perpendicular to the x-y-plane, Figure 1, with a 100 pixel overlap in the recorded images at x = 220 mm. The laser light sheet in the x-y plane is generated with a New Wave Gemini 200 mJ laser positioned in the middle of the channel (i.e. z = 0 mm). The liquid stream in the lower leg is tagged with Sulforhodamin G as a fluorescent dye. The fluorescent dye was injected with a variable speed syringe pump to maintain a sufficient dye density independent of the flow rate for all experiments. The LIF images were analyzed with DaVis V7.2 from LaVision. A spatial resolution of 0.25 mm is obtained, which

corresponds to one pixel. For all runs 1024 single frame, single exposure images were recorded and subsequently analyzed. Parameters for the experiments under consideration were the bulk inlet velocity, u_0, in the range from 0.2 m/s to 0.8 m/s and the relative density difference, $\Delta\rho$, from 0% to 10% between the two legs, Table 2.

4. Qualitative Flow Description

In the following section, qualitative observations in the flow field for both unstratified and stably stratified conditions are discussed. One instantaneous recording is selected from the recording sequence at each of the three velocities: 0.2 m/s, 0.4 m/s, and 0.8 m/s. For each velocity case, the unstratified (reference) condition is compared alongside stratified conditions for 1%, 3%, 5% and 10% relative density differences, Figures 2, 3, 4. These figures provide an initial impression of the developing mixing layer. The flow direction in each image is from left to right. The lower flow is tagged with Sulforhodamin G as a fluorescent dye and appears in white or gray scales, while the upper flow contains no dye and appears black.

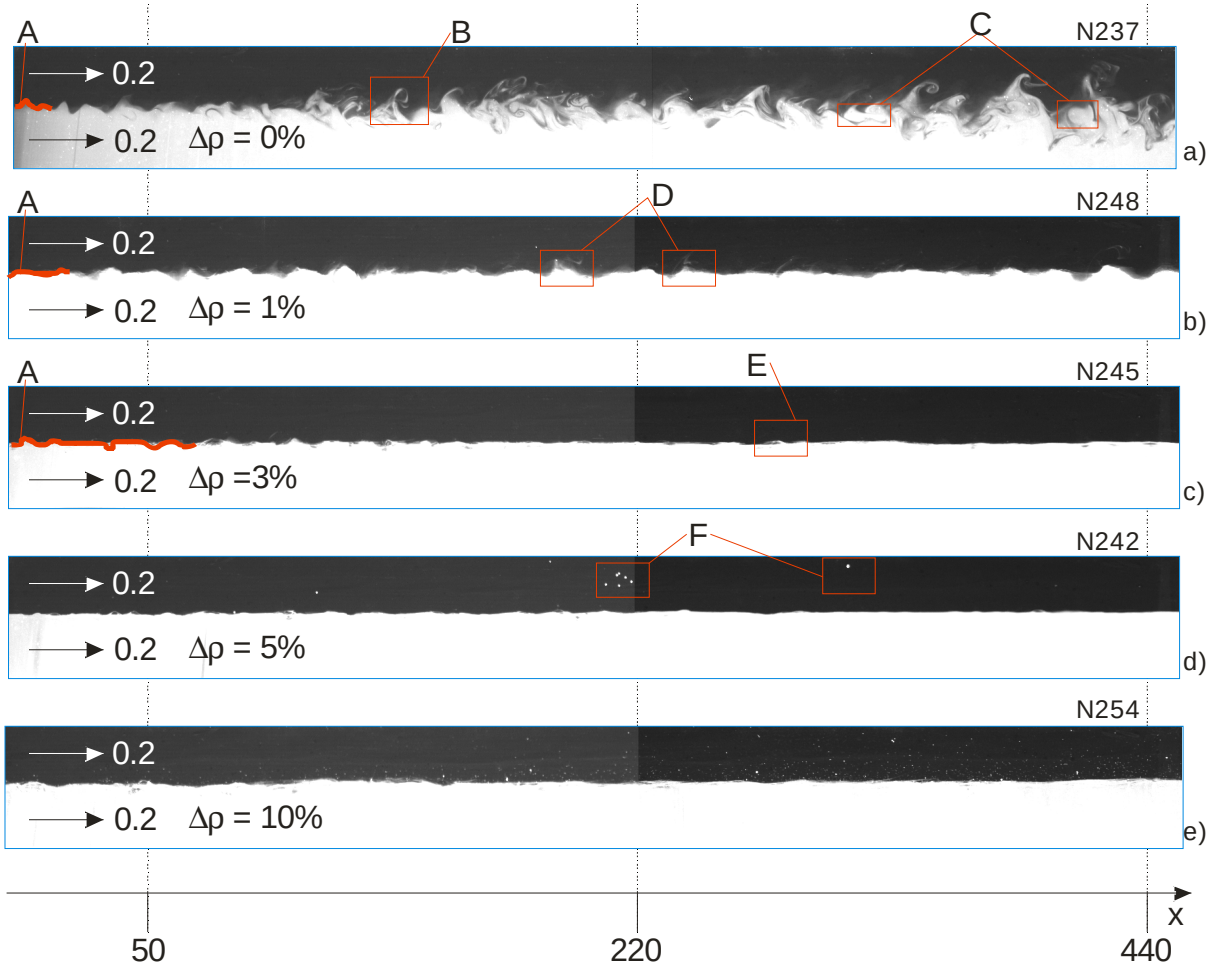

Figure 2: Instantaneous LIF-Images for 0.2 m/s inlet bulk velocity; a) unstratified (reference) case, b), c), d), e) relative density difference of 1%, 3%, 5% and 10%, respectively

The reference case for the inlet bulk velocity of 0.2 m/s is depicted in Figure 2 a). The initially compact instabilities (A) directly after the splitter plate tip grow continuously with downstream distance, and become less compact as indicated by the changing grey values. Due to isokinetic conditions, the centre of the mixing layers remains in the middle of channel. For x > 130 mm one can observe small clockwise rotating patterns (B) separating from the upper tip of the vortical structures. Further downstream, in the range between 300 mm and

400 mm, the formation of compact closed structures or clusters (C) becomes visible. Due to a slight overexposure in the images the aforementioned structures are not visible in the lower part. For the case with 1% relative density difference the initially small instabilities (A) generate only a wavy pattern at the interface between the two streams, and on some parts of the wave peaks small structures separate (D), Figure 2 b). Compared with the previous result, the growth of the mixing zone is already considerably suppressed such that between 250 < x <380 mm the wavy interface pattern reduces to a flat line, however this increases again downstream of 380 mm. For the 1% stratification case some separations on the top of the wave peaks (D) also become visible. For the 3% case, the initially small instabilities (A) remain the same in the range up to 150 mm and nearly no mixing is observed, Figure 2 c). For x > 150 the wavy pattern is damped out, indicating that the mixing in the mixing zone is widely suppressed and the interface between the two fluids can be approximated by a horizontal line. What remains are only a few very small flow separations (E). For 5% density difference the activity in the mixing zone vanishes completely, Figure 2 d). The white spots (F) appearing at random in the upper part of the channel were identified as particle clusters from previous PIV measurements; these particles are successively re-entrained from channel surfaces and appear now in the LIF measurements.

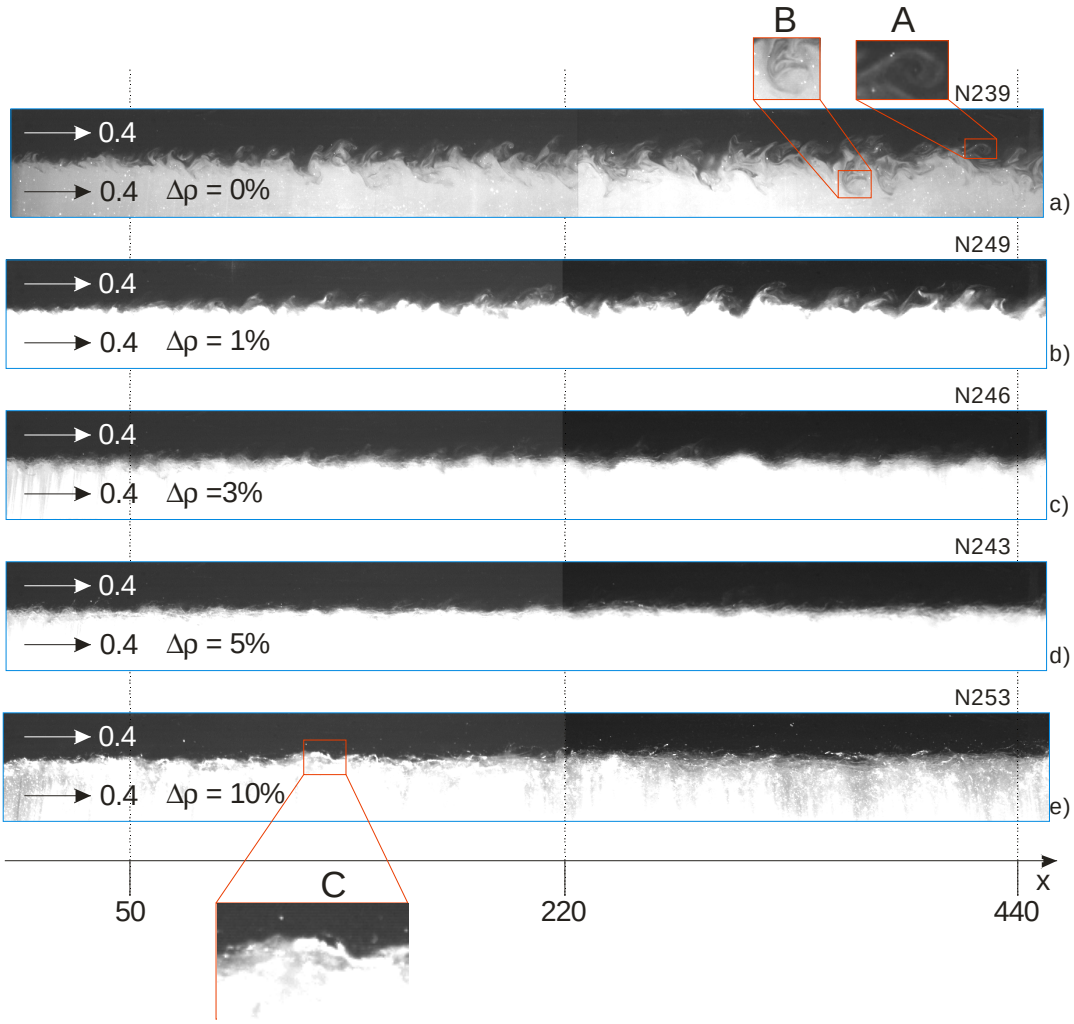

Figure 3: Instantaneous LIF-Images for 0.4 m/s inlet bulk velocity; a) unstratified (reference) case, b), c), d), e) relative density difference of 1%, 3%, 5% and 10%, respectively

For an inlet bulk velocity of u_0=0.4 m/s, again vortex structures can be observed for the unstratified reference case as well as for the case with 1% density difference, Figure 3a). The latter is in contrast to the experiments with 0.2 m/s, in which no vortex structures were visible at 1% density difference. What may be found similar to the 0.2 m/s case is the presence of

clockwise rotating structures (A), which separate from the wave peaks in the upper half of the channel. Also, the appearance of counterclockwise rotating structures (B) in the lower half of the channel is noted, Figure 3 a); these were not visible for the 0.2 m/s cases. For a density difference of 3%, the typical shaped vortex structures disappear and instead a wavy pattern becomes visible again.
The reference case for 0.8 m/s shows again the typical shaped vortex structures. But in relation to the cases with 0.2 and 0.4 m/s, the structures are smaller and less regular in space, Figure 4 a). The case with 1% stratification shows also some typical vortex structures, but the interface between the two streams is sharper than in the reference case and the mixing layer growth is slower, Figure 4 b). With 3% density difference one can observe that in a range up to 100 mm the mixing zone shows only very few small waves, which increase further downstream in number and amplitude, Figure 4 c). Also, the formation of lamellas which separate from the wave peaks can be localized in the case with 3% density difference. Similar to the 3% case, we find for the 5% case a relatively free boundary layer in the range of up to 100 mm, Figure 4 d). In fact, further downstream the number of waves increases but not the amplitudes of these waves. Additional attention should be given to the white spots (A), which appear in the upper part of the channel in the 5% stratified case, Figure 4 d). These bright spots are clusters of pure, unmixed fluid which appear to have erupted out of the higher density portion tagged with the dye. This finding is supported by the situation that several of these relatively large bright spots (A) can be found in the upper stream. This topic requires further investigation.

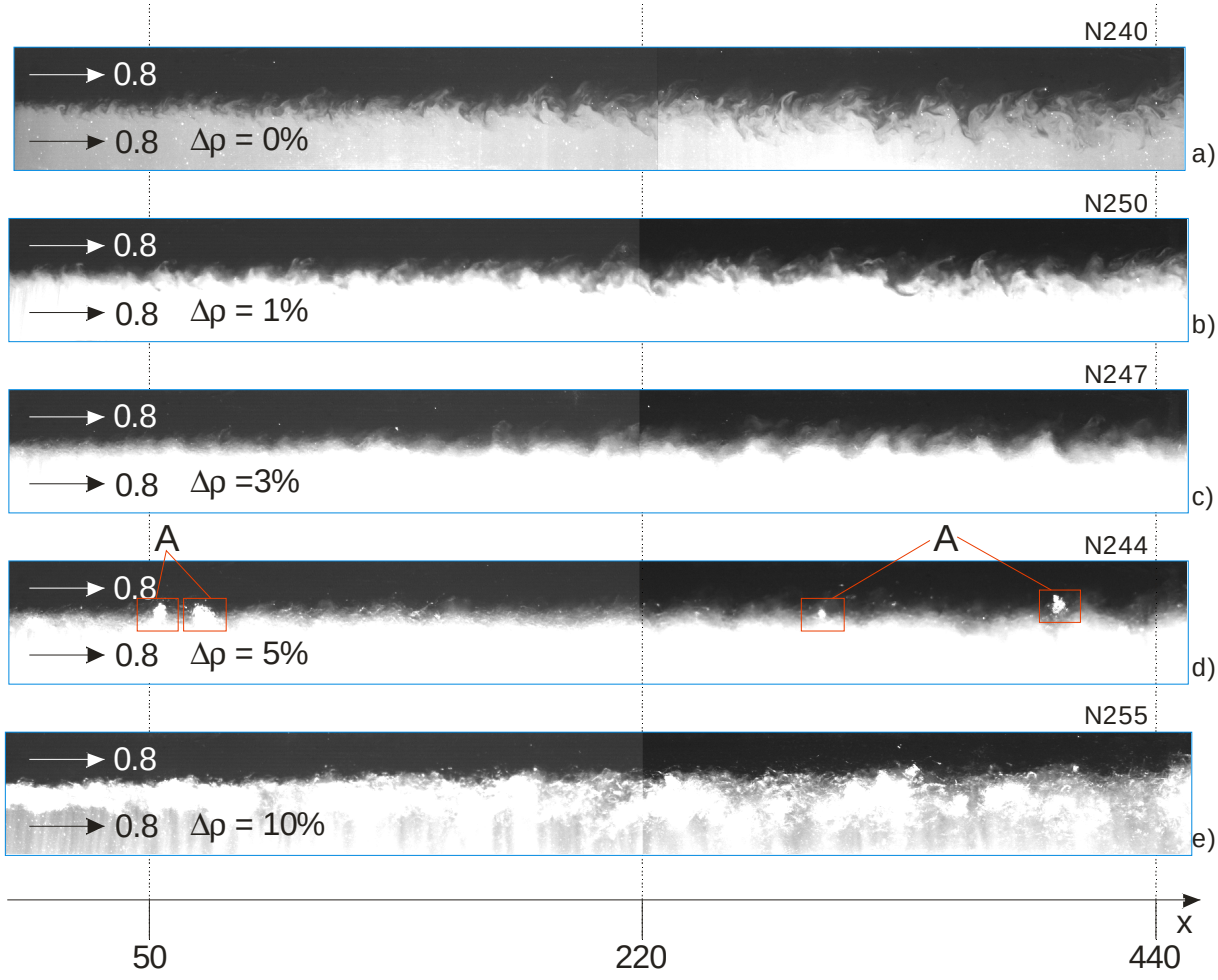

Figure 4: Instantaneous LIF-Images for 0.8 m/s inlet bulk velocity; a) unstratified (reference) case, b), c), d), e) relative density difference of 1%, 3%, 5% and 10%, respectively

5. Semi-Quantitative Flow Description

The following section will work to present the observed results in an approximate or semi-quantified manner. The analysis applied to the LIF measurements will be explained in further detail, including the use of fit functions in determining necessary coefficients for proving the self-similarity of the concentration field of the resultant mixing layer.

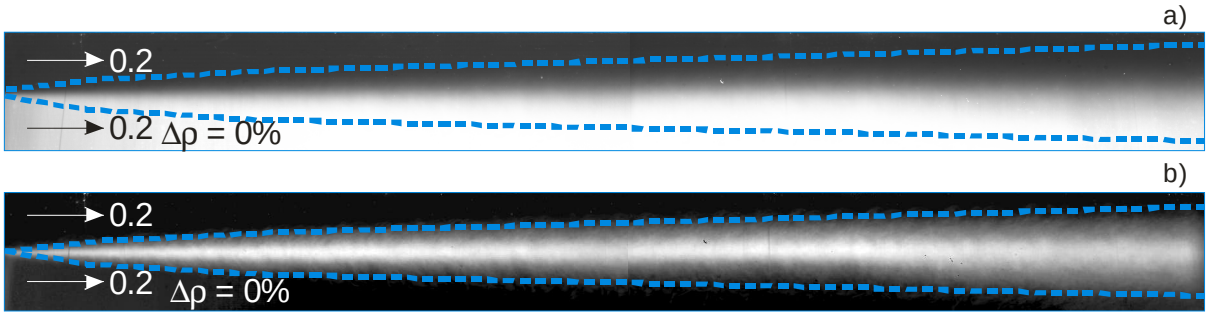

Figure 5: Averaged a) and rms b) image out of 1024 instantaneous LIF-image recordings

In the LIF data processing 1024 images are averaged to obtain a visualization of the developing mixing layer, Figure 5. The dashed lines in the above Figure outline the growth of an approximate mixing layer. The images obtained through LIF are taken at 8 bit grayscale resolution depth, with the upper limit (no dye visible) appearing as black and assigned a value of approximately 0, and the lower limit (completely dyed) appearing as white with an assigned value of approximately 255.
This averaged image is then used for the extraction of vertical concentration profiles at varying downstream locations. The gray scale values of the individual profiles are then normalized to a scale between 0 and 1 for the purpose of our data analysis. On this scale, a value of 0.5 indicates a perfectly mixed region.

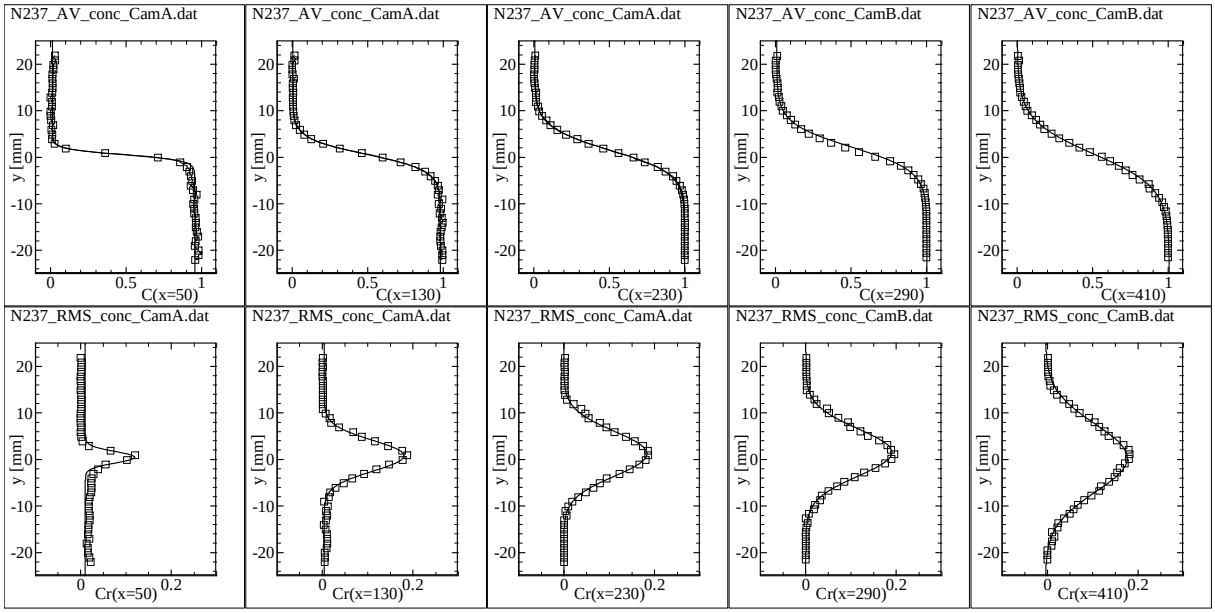

Figure 6: Mean values in different distances downstream of the splitter plate tip (upper plots); rms values in different distances downstream of the splitter plate tip (lower plots) for experimental run N237 with u_0 = 0.2 m/s without stratification (reference case)

The extracted profiles indicate the level of mixing occurring, and serve to identify with more precision the development of the mixing layer between the two streams. rms profiles are also extracted from the image to quantify the fluctuations of the mean concentration values

throughout the layer. This is done using the analyzer software DaVis V7.2 from LaVision. A sample of these concentration and rms profiles for the unstratified case N237 is displayed in the lower part of Figure 6. The upper graphs plot the normalized mean concentration values, C, between 0 and 1, versus the vertical distance, y, from the splitter plate tip, ±25 mm, for different downstream distances indicated below the plots, C(x=130) for example. The lower plots represent the normalized rms values, C_r, on the x-axis, plotted again against the vertical distance on the y-axis at the same downstream distances. The individual points on each plot represent respective values taken from the grayscale of the averaged LIF image. For the presented case, it is observed that the mixing zone appears to grow with downstream distance. As a first order approximation, arbitrary boundary values of 0.1 and 0.9 were selected for the normalized concentration as a mixing range. It is visible that the vertical range over which the normalized concentration falls between these values increases with increasing downstream distance. A similar phenomenon is observed in the case of the rms value profiles; it is noted that the vertical range over which the normalized rms values fall above the arbitrarily chosen value of 0.05 increases with increasing downstream distance, indicating again the growth of the mixing layer. These criteria for the mixing layer thickness are further refined through the introduction of fit functions below.
Based on the research of Townsend 1976, we check for the self-similarity of the experimental results. The data points for the mean concentration values are fitted with a hyperbolic tangent function which was selected due to its similarity to the error function.

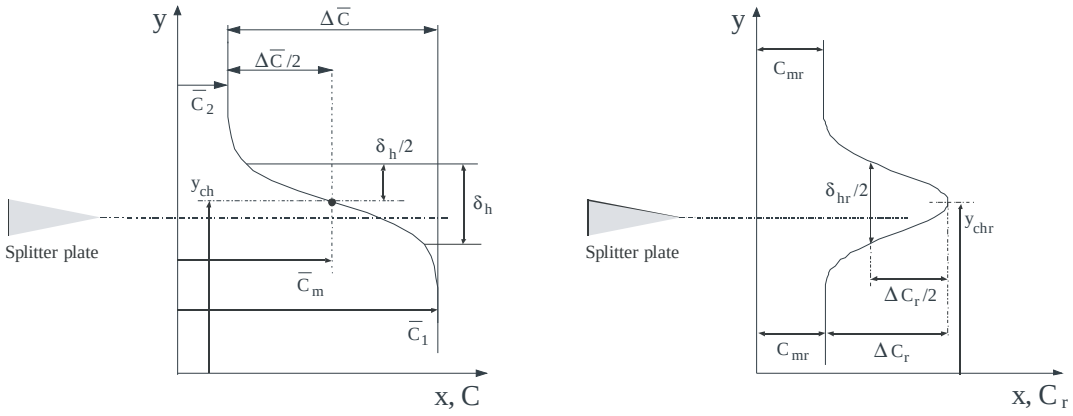

Figure 7: Schematic for the variables used for the fit functions

$$\bar{C}_{(x,y)} = \bar{C}_m - \frac{\Delta \bar{C}}{2} \cdot \tanh\left(\frac{y - y_{ch}}{\delta_h / 2}\right) \qquad \text{Eq. 1}$$

In this equation, $\bar{C}_m$ denotes the 50% concentration value (also the point of inflection of the curve) and $\Delta\bar{C}$ is the maximum change in concentration, Figure 7. The variable y denotes height measured from the centerline of the channel, whereas y_{ch} denotes the difference between the centerline of the channel and the center of the profile. Finally, δ_h denotes the width of the mixing layer, with a value ranging between 0.1 and 0.9.
The rms data points are then fitted with a Gaussian normal distribution curve, again selected based on similarity to the error function.

$$\bar{C}_{rms(x,y)} = \bar{C}_{mr} + \Delta\bar{C}_{rms} \cdot \exp\left[-\left(\frac{y - y_{chr}}{\delta_{hr} / 2}\right)\right] \qquad \text{Eq. 2}$$

Here, $\overline{C}_{mr}$ denotes the minimum rms value (offset) and $\Delta\overline{C}_{rms}$, the maximum change in rms. The variable y again denotes height measured from the centerline of the channel, while y_{chr} denotes the difference between the centerline of the channel and the peak of the curvature. Similar to the previous equation, δ_{hr} denotes the width of the mixing layer.
From the application of Eq. 1 and 2 to the plots seen above, the arguments of the hyperbolic tangent function as well as the arguments of the exponential function are extracted. The values of the coefficients comprising both of these expressions are solved for, and then used to define similarity variables for each case:

$$\left.\begin{aligned}\eta &= \frac{C - C_m}{\Delta C / 2}\\ \zeta &= \frac{y - y_{ch}}{\delta_h / 2}\end{aligned}\right\} \overline{C} \qquad \text{Eq. 3}$$

$$\left.\begin{aligned}\eta_r &= \frac{C_r - C_{mr}}{\Delta C_r / 2}\\ \zeta_r &= \frac{y - y_{chr}}{\delta_{hr} / 2}\end{aligned}\right\} \overline{C}_{rms} \qquad \text{Eq. 4}$$

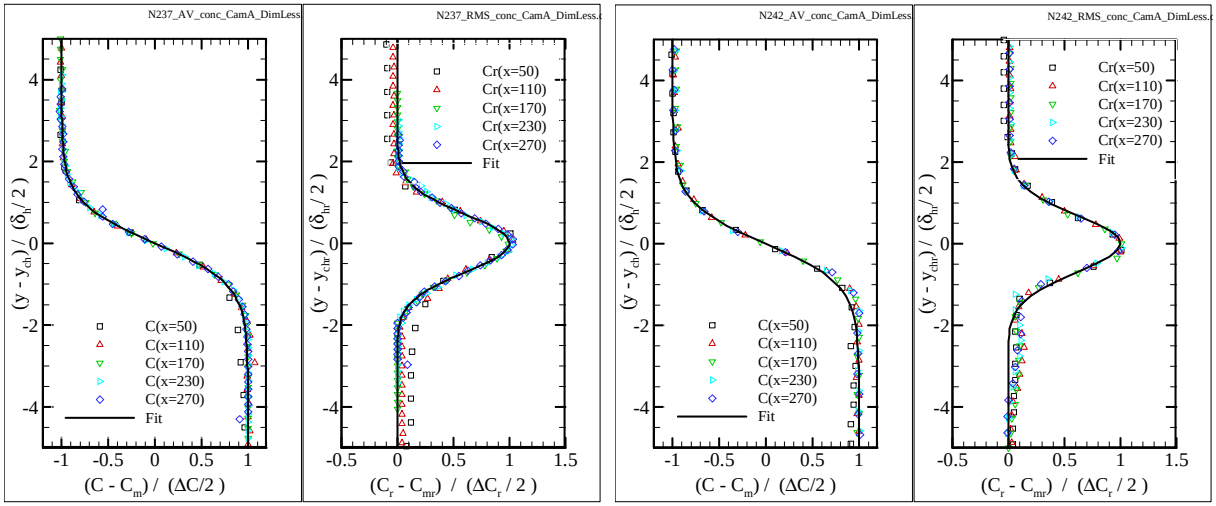

Figure 8: Self similarity presentation of the normalized concentration field approach for mean and rms for u_0 = 0.2 m/s a) reference case without stratification b) stratified case with 5% relative density difference.

The coefficients described above are then calculated for various downstream distances and plotted in order to visualize the self-similarity of the data, Figure 8. The calculated value for ζ is plotted on the y-axis versus η along the x-axis. The left plot a) represents the unstratified (reference) case, and the right plot b) represents the stratified case (5% relative density difference), both at an inlet bulk velocity of 0.2 m/s.
For lower downstream distances it is found that the data points fall more in line with one another within the mixing region, and drift further away from the self-similarity line closer to the upper and lower walls. Additionally, self-similarity appears to improve with increased downstream distance. It is also noted that the mean concentration values attain self-similarity earlier than the rms values.
Upon detailed examination of the plots for the stratified case we see that the data points are less accurately in line with the self-similarity curve, particularly in the lower half of the channel for the rms plot, Figure 8 b). Furthermore, an increased gradient of the self-similarity line is noted in the lower half of the channel as compared to the curve in the upper half. A possible explanation for this is discussed further in Baker 1968, relating this phenomenon to the effect of the gravitational body force on the higher density (lower) fluid. Differently spoken, it appears that more mixing occurs from the upper stream to the lower stream than vice versa.

This observation is further supported by concentration measurements taken with a wire mesh sensor, Fokken 2010.

6. Conclusions

In this experiment LIF measurements were performed, and collected data was processed and checked for self-similarity. LIF images were first examined qualitatively, and the change of the vortex structures typical of the unstratified cases into lamella type structures for strong stratification was observed. A semi-quantitative approach was then pursued, with the normalization of the 8 bit LIF images to a 0 to 1 intensity grayscale for the purpose of more detailed comparison. Through this analysis it was found that self-similarity is attained in both the unstratified reference case as well as in a moderately (5% density difference) stratified case. With increased stratification (10% density difference), the deviation of the data from self-similarity grows. It was also seen that self-similarity is attained earlier for the mean concentration values than for the rms values. Additionally, a steeper gradient was observed for the lower half of the channel compared with the upper half in the stratified case, however this topic still requires further investigation. Future experiments and analysis will include testing at a variety of velocities to check if self-similarity is also independent of velocity.

Acknowledgements

The authors would like to thank AXPO AG, Division Kernenergie (formerly Nordostschweizerische Kraftwerke AG) Nuclear Power Plant Beznau, KKB for financial support in the GEMIX-Experiments and supporting of the Ph.D. studies.

7. Reference

Chapuliot, S., Gourdin, C., Payen, T., Magnaud, J.P., Monavon, A.: "Hydro-thermal-mechanical analysis of thermal fatigue in a mixing tee", Nuclear Engineering and Design 235 (2005), 575-596

Metzner, K.-J., Wilke, U.: "European THERFAT project – thermal fatigue evaluation of piping system "Tee"-connections", Nuclear Engineering and Design 235 (2004), 473-484

Walker, C., Simiano, M., Zboray, R., Prasser, H.M.: "Investigations on mixing phenomena in single-phase flow in a T-junction geometry", Nuclear Engineering and Design 239 (2009), 116-126

Prasser, H.M., Böttger, A., Zschau, J.: A new electrode-mesh tomograph for gas-liquid flows", Flow measurement and instrumentation, 9 (1998), 111-119

Kapulla R., Dyck, C., Witte, M., Fokken, J., Leder, A. (2009):"Optical Flow and Cross Correlation Techniques for Velocity Field Calculation", Fachtagung "Lasermethoden in der Strömungsmesstechnik", 8.-10. September 2009, Erlangen

Fokken, J., Kapulla, R., Kuhn, S., Dyck, C., Prasser, H.M. (2009): "Stably stratified isokinetic turbulent mixing layers: Comparison of PIV-measurements and numerical calculations", Fachtagung "Lasermethoden in der Strömungsmesstechnik", 8.-10. September 2009, Erlangen

Fokken, J., Kapulla, R., Galgani, G., Schib, O., Prasser, H.M. (2010): “Stably stratified isokinetic turbulent mixing layers – Investigations in a square flow channel”; Proceedings of the IYNC 2010

Townsend 1976: „Monographs on Mechanics and Applied Mathematics, 2nd Edition“; Cambridge University Press

Baker, R. L.; Weinstein, H. 1968: “Velocity and density profiles in mixing region between adjacent half jets of dissimilar fluids”; Report Number: NASA-CR-957